ATLAS Note
GROUP-2021-XX
14th December 2022
Draft version 0.1

ATLAS Liquid Argon electromagnetic calorimeter shower shape study with the cross-talk and detector geometry

The ATLAS Collaboration

This note presents the study on the impact from cross talk and detector geometry description to the shower shape in ATLAS Liquid Argon (LAr) electromatic calorimeter. Single photon events in several $|\eta|$ points within the calorimeter barrel region are used. They are simulated with different detector descriptions, and digitalized with a set of scale values applied on the cross talk amplitude. Some defined shower shape variables commonly used in ATLAS photon identification are selected to present the impact. The impact from cross talk is significant and has the potential to match the η direction shower shape in data. Considered geometry descriptions shows little difference on the shower shape variables and can not be the reason for the shower shape mismodeling in the simulation.

Contents

1 Introduction

In the ATLAS detector, the Liquid Argon electromagnetic calorimeter (LAr ECAL) is used to measure the electromagnetic (EM) showers from photons and electrons. It is a sampling calorimeter with accordion-shaped kapton electrodes and lead absorber plates over its full coverage. Longitudinally it is divided 3 layers, plus one additional pre-sampling layer. The lateral segmentation varies in layers. This granularity allows us to extract the shape of EM showers and use them to identify particles. Currently in ATLAS the photon identification (ID) is through a cut-based method on several discriminating variables derived from the particle shower shapes [1]. Optimizing this photon ID is essential to the photon-related physics analysis in the ATLAS, e.g. $H \rightarrow \gamma\gamma$ studies.

However, it is known that ATLAS simulation does not predict the photon and electron shower developments in the ECAL perfectly, especially in the lateral profile. There is a data-driven correction to these shower shape variables for the photon ID. The central values and widths of the distributions are shifted to match the values in data, normally known as "fudge-factor" method. And its influence is considered as a term of systematic uncertainty in the physics analysis.

The reason of this disagreement can come from many aspects:

- Geometry description before the LAr ECAL and the LAr ECAL. The material before active part of LAr calorimeter can increase the possibility of showering. The values of LAr ECAL geometry description, e.g. the thickness of lead absorber board, material composition, sensitive LAr cell size, have direct relation to the calorimeter radiation length and the effective Moliere radius. Also 10 years after the ATLAS construction they can have variations due to gravity, temperature, aging.
- Charge collection effects in the simulation. The electromagnetic shower development and energy deposition of each step are simulated by Geant4 [2]. The electric field map in the LAr gap, energy sharing across cells from electric field effect and saturation effects are possible to introduce some disagreement.
- Detector digitization. The cross-talk and electronic noise in the readout can change the signal from cells and contaminate the shower shapes.

Many efforts were made previously. In 2010 part of the disagreement was mitigated by transiting to the detailed LAr accordion simulation from the blended material. Several checks on the simulation are done and are proved negligible. In this note we investigate the effects from cross talk and LAr structure. It is organized as follows. A brief introduction to the ATLAS LAr ECAL and the shower shape variables used in the photon ID is given in Section 2. Section 3 lists the configurations of cross-talk in the digitalization and their impact to the shower shapes. Section 4 we talk about some kinds of mismodeling of LAr ECAL, and check the shower shapes again. Results and conclusions are given in Section 5.

2 ATLAS LAr electromagnetic calorimeter and shower shapes

The ATLAS LAr EM calorimeter is divided into a barrel section (EMB) covering the pseudo-rapidity region $|\eta| < 1.475$, and two endcap sections (EMEC) covering $1.375 < |\eta| < 3.2$. In the region $|\eta| < 2.5$ it is separated into three layers. The first layer, also called strip layer, is the most granular of the three ($\Delta\eta \times \Delta\phi = 0.003 \times 0.1$) to provide an event-by-event discrimination between single-photon showers and overlapping showers. The second layer collects most of the energy deposited in the calorimeter by EM showers, has a thickness of about 17 X_0 and a granularity of $\Delta\eta \times \Delta\phi = 0.025 \times 0.025$. The third layer, which has a granularity of $\Delta\eta \times \Delta\phi = 0.05 \times 0.025$, is used to correct for leakage beyond the EM calorimeter for high-energy showers. Figure 2.1 gives sketch of a barrel module of ATLAS EM calorimeter.

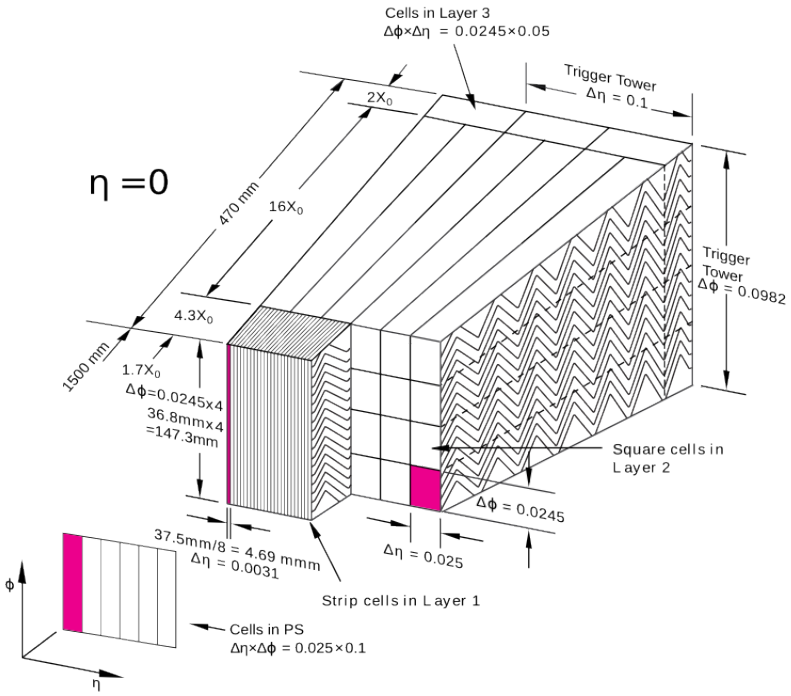

Figure 2.1: Sketch of a barrel module of ATLAS LAr EM calorimeter.

The photon is reconstructed from the dynamic topological clusters in the calorimeter. After the clusters are formed, some shower shape variables are calculated for the photon and electron identification, as listed in Table 2.1.

Category	Description	Name
Hadronic leakage	Ratio of E_T in the first layer of the hadronic calorimeter to E_T of the EM cluster (used over the ranges $\|\eta\| < 0.8$ and $\|\eta\|.1.37$)	R_{had1}
	Ratio of E_T in the hadronic calorimeter to E_T of the EM cluster (used over the range $0.8 < \|\eta\| < 1.37$)	R_{had}
EM second layer	Ratio of the sum of the energy of the cells contained in a $3 \times 7\eta \times \phi$ rectangle(measured in cell units) to the sum of the cell energies in a 7×7 rectangle, both centred around the most energetic cell	R_η
	Lateral shower width, $\sqrt{((\Sigma E_i \eta_i^2)(\Sigma E_i) - ((\Sigma E_i \eta_i)(\Sigma E_i))^2)}$, where E_i is the energy and η_i is the pseudorapidity of cell i and the sum is calculated with a window of 3×5 cells	$w_{\eta 2}$
	Ratio of the sum of the energies of the cells contained in a $3 \times 3\eta \times \phi$ rectangle(measured in cell units) to the sum of the cell energies in a $3 \times 7\eta \times \phi$ rectangle, both centred around the most energetic cell	R_ϕ
EM first layer	Total lateral shower width, $\sqrt{(\Sigma E_i (i - i_{max})^2)(\Sigma E_i)}$, where i runs over all cells in a window of $\Delta\eta \approx 0.0625$ and i_{max} is the index of the highest-energy cell	w_{stot}
	Lateral shower width, $\sqrt{(\Sigma E_i (i - i_{max})^2)(\Sigma E_i)}$ where i runs over all cells in a window of 3 cells around the highest-energy cell	$w_{s3}/w_{\eta 1}$
	Energy fraction outside core of three central cells, within seven cells	f_{side}
	Difference between the energy of the cell associated with the second maximum, and the energy reconstructed in the cell with the smallest value found between the first and second maxima	ΔE_s
	Ratio of the energy difference between the maximum energy deposi and the energy deposit in a secondary maximum in the cluster to the sum of these energies	E_{ratio}
	Ratio of the energy measured in the first layer of the electromagnetic calorimeter to the total energy of the EM cluster	f_1

Table 2.1: Discriminative shower shape variables used for photon identification.

3 Cross-talk impact to the shower shapes

The cross-talk effect describes the signal leakage in the calorimeter cell introduced from or to its neighbor cells. It is caused by capacitive, resistive or inductive coupling between calorimeter cells and observed as a pulse distortion in the cell. This effect leads to the change to the signal amplitude in the calorimeter cell, and then influences the reconstructed cluster energy and the shower shapes. In ATLAS the cross-talk effect is firstly studied in the calibration run by pulsing one cell and observing the induced signal shapes in the nearby cells [3, 4]. A complete map of the cross-talk in the detector was provided and implemented into the digitization of MC simulation. But some discrepancies were observed when comparing the map with the data with $Z \rightarrow \mu\mu$ process [5]. Start from this point, we first check how much impact these discrepancies can bring to the shower shapes.

In the ATLAS LAr digitization, the cross-talk amplitude within the LAr layers can be globally scaled. Based on this a set of photon particle gun events are simulated by Geant4 [2]. Photon energy is fixed to 65.536 GeV. Four $|\eta|$ points are selected to check the η-dependency: $|\eta| \in [0.2, 0.25]$, $|\eta| \in [0.5, 0.55]$, $|\eta| \in [0.95, 1]$, $|\eta| \in [1.2, 1.25]$. The simulation follows the default settings in ATLAS, with the detector description *ATLAS-R2-2016-01-00-01*, Geant4 version 10.1 and the physics list *FTFP_BERT_ATL*. As a comparison, another physics list *FTFP_BERT_EMZ* with Geant4 version 10.6 is used. This is believed as the best description of the electromagnetic physics models selected from the low energy and standard packages. Details are summarized in Table 3.1.

Process	Single photon
DSID	431004, 431010, 431019, 431024
Energy	65.536 GeV
$\|\eta\|$	[0.20, 0.25], [0.50, 0.55], [0.95, 1.00], [1.20, 1.25]
ϕ	$[0, 2\pi]$
Geometry	*ATLAS-R2-2016-01-00-01*
Geant 4 version and physics list	10.1 + *FTFP_BERT_ATL* 10.6 + *FTFP_BERT_EMZ*
Statistics	1000

Table 3.1: Configuration of simulated samples.

To cover the uncertainties of cross talk measurement, 3 configurations are applied in the amplitude scale:

- Central scale: the scale factor is derived from the cross talk value in data over the value in the map of digitization.
- Lower scale: the factor is derived from the upper edge of the cross talk value uncertainty of MC simulation over the lower edge of the uncertainty of data.
- Upper scale: on the contrary of lower scale, the factor is derived from the lower edge of the cross talk value uncertainty of MC simulation over the upper edge of the uncertainty of data.

		$\|\eta\| \in [0.20, 0.25]$	$\|\eta\| \in [0.50, 0.55]$	$\|\eta\| \in [0.95, 1.00]$	$\|\eta\| \in [1.20, 1.25]$
Strip layer	Central	1.174	1.222	1.737	1.780
	Lower	1.000	1.000	1.160	1.224
	Upper	1.289	1.477	1.974	2.361
Middle layer	Central	1.600	1.939	2.015	1.256
	Lower	1.102	1.027	1.241	1.056
	Upper	3.267	2.533	2.800	2.217

Table 3.2: Cross talk scale values in 3 configurations.

It is believed the needed scale value is between the lower and upper value. Scale values are listed in Table 3.2.

After the generation and digitization the photon is reconstructed following the standard reconstruction algorithm. Unconverted photons are selected. Four shower shape variables, $w_{\eta 1}$, $w_{\eta 2}$, R_η and R_ϕ are considered to study the cross-talk impact. Figure 3.1 shows the distribution of these 4 shower shape variables in η point $|\eta| \in [0.2, 0.25]$. Their mean values are extracted and visualized in Figure 3.2. These results show the cross-talk can have significant impact to the η-related shower shapes like R_η, $w_{\eta 1}$, $w_{\eta 2}$, and can have very little influence to the ϕ direction, which is also as expected because the accordion structure ensures the cross-talk in ϕ is negligible.

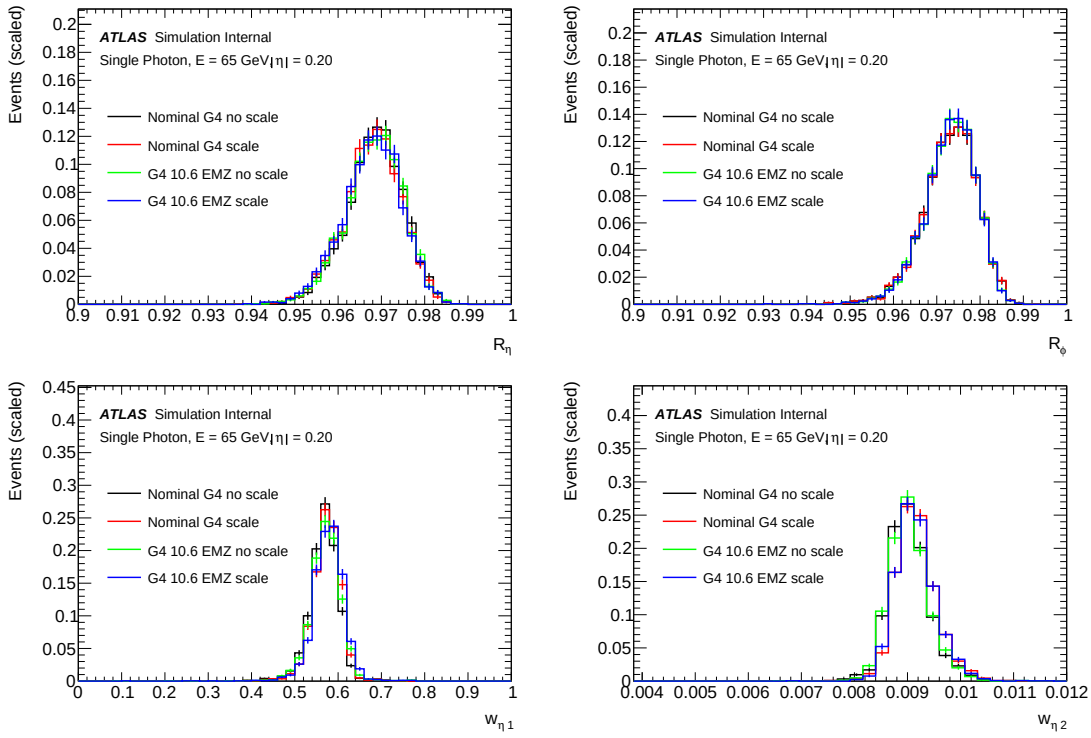

Figure 3.1: Distribution of shower shape variables

To illustrate the relationship between the cross talk amplitude and the η-related shower shape variables, the scale values and shower shape mean values are visualized in Figure 3.3 and fitted with a linear function, separately for the strip layer and middle layer. The linear relationship is quantified with $r^2 = 1 - \frac{\Sigma_i (\hat{y}_i - y_i)^2}{\Sigma_i (\bar{y}_i - y_i)^2}$.

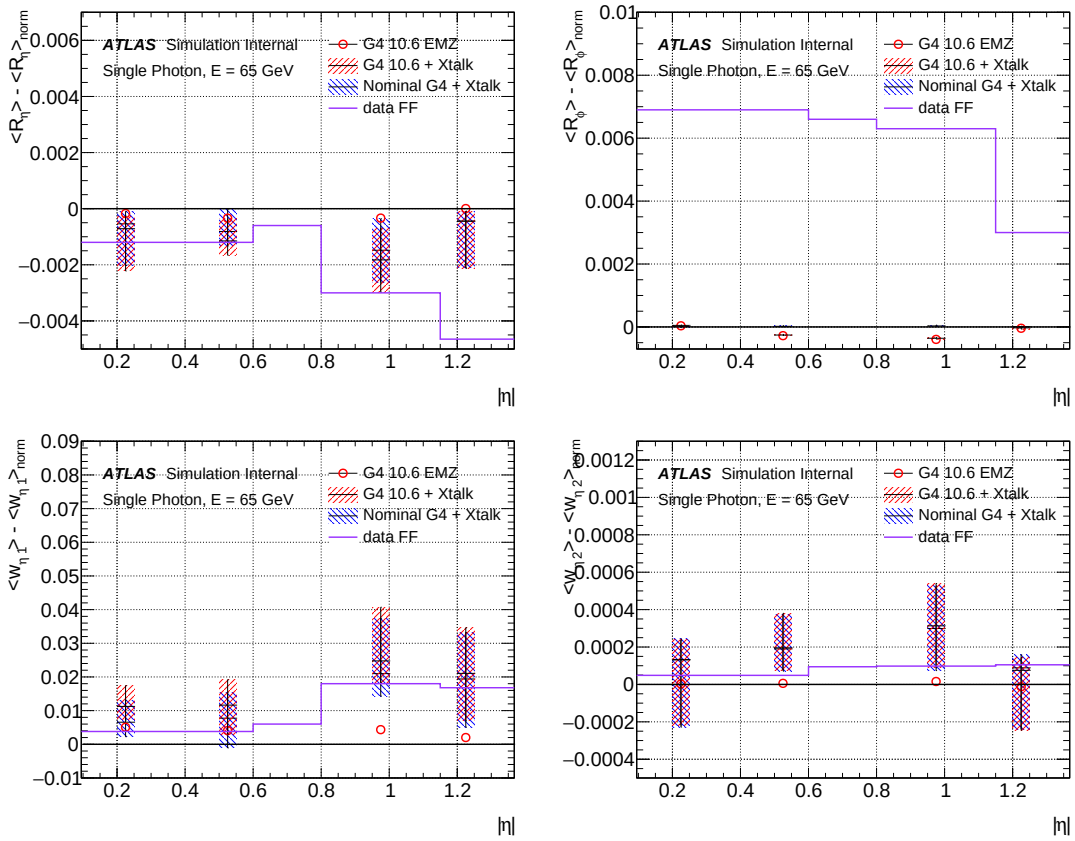

Figure 3.2: Mean values of shower shape variables with $|\eta|$-dependence. The nominal ATLAS simulation is used as reference. The impact from upper and lower scale cross talk (Xtalk) values is shown as the bondary of uncertainty band.

Results here show $w_{\eta 1}$, w_{stot} and f_{side} can always have a good linear relationship with the strip layer cross talk ($r^2 > 0.999$), same for R_η and $w_{\eta 2}$ with the second layer cross talk. Based on this an attempt to extract the needed cross-talk value from the data is made and shown in Figure **??** and Table **??**. The obtained cross-talk values from several shower shape variables are not consistent, meaning through the cross-talk we can not fix all the disagreement in shower shapes.

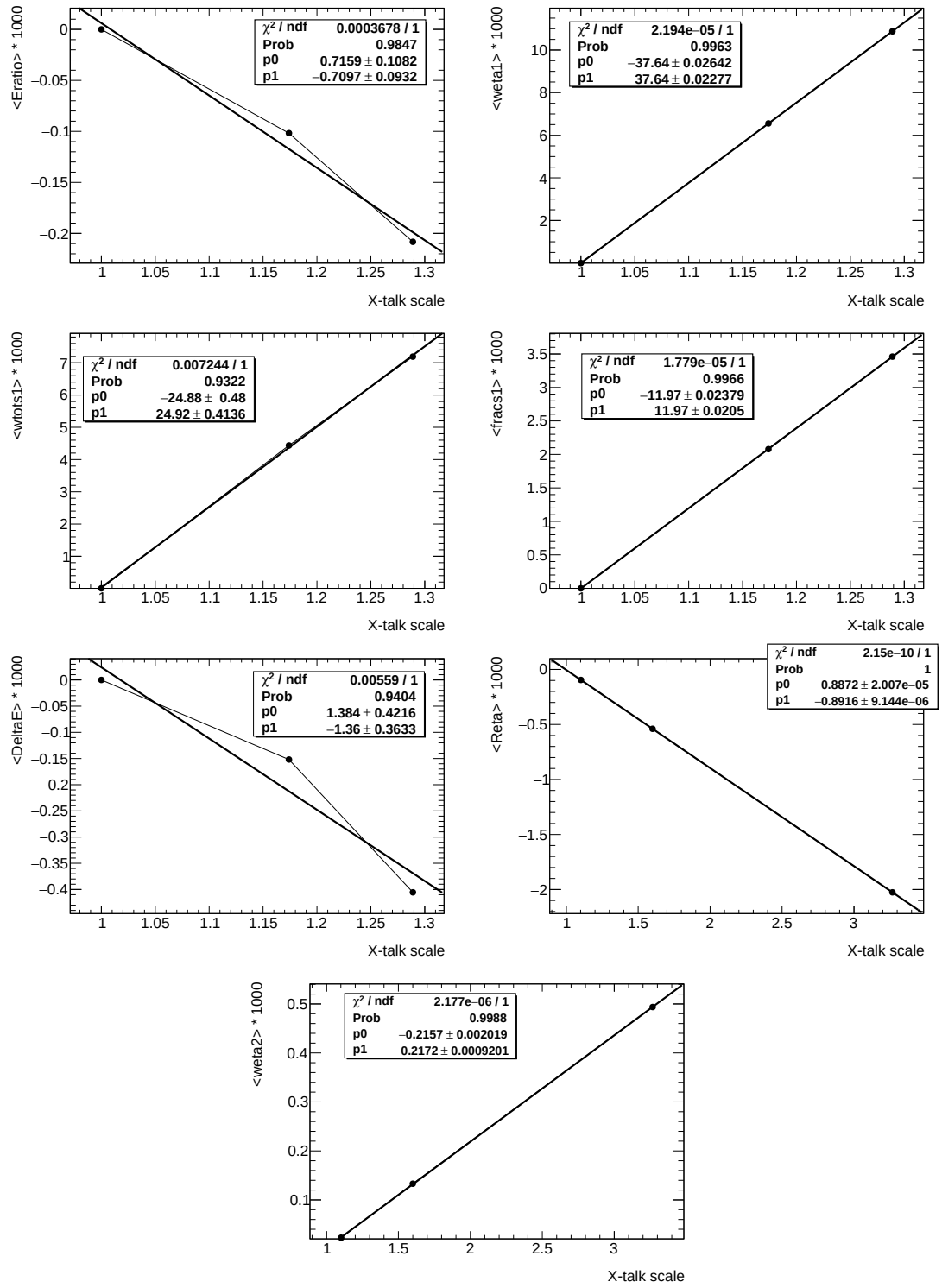

Figure 3.3: The cross talk scale value and shower shape variable mean value relationship at $|\eta|$ range [0.20, 0.25]. Three points corresponds to the lower/central/upper scale and are fitted with a linear function.

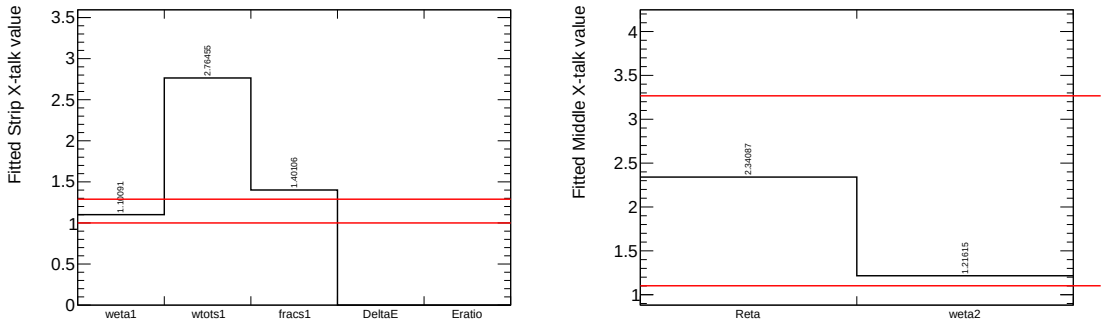

(a) Strip layer (b) Middle layer

Figure 3.4: Fitted cross talk value from shower shape variables in strip layer (left) and middle layer (right) in $|\eta| \in [0.20, 0.25]$. Red lines are the upper and lower range from the cross talk measurement, i.e. the lower and upper scale values.

	Data FF	Fitted x-talk	r^2
$w_{\eta 1}$	0.004	1.101	1.00
w_{stot}	0.044	2.764	1.00
f_{side}	0.005	1.401	1.00
ΔE	0.000	-	0.93
E_{ratio}	0.002	-	0.98
R_{η}	-0.001	2.341	1.00
$w_{\eta 2}$	0.000	1.216	1.00

Table 3.3: The data fudge factor, the fitted cross talk amplitude scale values from the fudge factor and the linear relationship of different shower shape variables in $|\eta| \in [0.20, 0.25]$. The fitted cross talk scale values in the first 5 rows refers the first layer scales, and the last 2 are the middle layer scales. The fit is performed only for the variables with $r^2 > 0.999$.

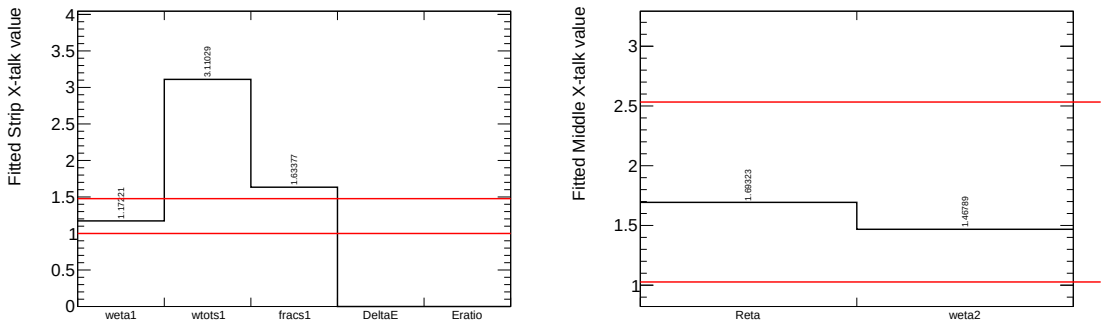

(a) Strip layer (b) Middle layer

Figure 3.5: Fitted cross talk value from shower shape variables in strip layer (left) and middle layer (right) in $|\eta| \in [0.50, 0.55]$. Red lines are the upper and lower range from the cross talk measurement, i.e. the lower and upper scale values.

	Data FF	Fitted x-talk	r^2
$w_{\eta 1}$	0.006	1.172	1.00
w_{stot}	0.047	3.110	1.00
f_{side}	0.008	1.634	1.00
ΔE	0.000	-	0.99
E_{ratio}	0.000	-	0.97
R_{η}	-0.001	1.693	1.00
$w_{\eta 2}$	0.000	1.468	1.00

Table 3.4: The data fudge factor, the fitted cross talk amplitude scale values from the fudge factor and the linear relationship of different shower shape variables in $|\eta| \in [0.50, 0.55]$. The fitted cross talk scale values in the first 5 rows refers the first layer scales, and the last 2 are the middle layer scales. The fit is performed only for the variables with $r^2 > 0.999$.

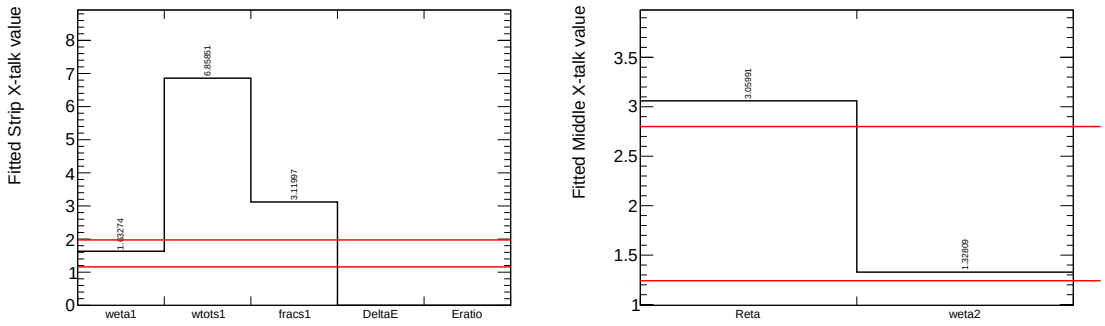

(a) Strip layer

(b) Middle layer

Figure 3.6: Fitted cross talk value from shower shape variables in strip layer (left) and middle layer (right) in $|\eta| \in [0.95, 1.00]$. Red lines are the upper and lower range from the cross talk measurement, i.e. the lower and upper scale values.

	Data FF	Fitted x-talk	r^2
$w_{\eta 1}$	0.018	1.633	1.00
w_{stot}	0.100	6.859	1.00
f_{side}	0.022	3.120	1.00
ΔE	0.000	-	0.93
E_{ratio}	-0.003	-	0.98
R_{η}	-0.003	3.060	1.00
$w_{\eta 2}$	0.000	1.328	1.00

Table 3.5: The data fudge factor, the fitted cross talk amplitude scale values from the fudge factor and the linear relationship of different shower shape variables in $|\eta| \in [0.95, 1.00]$. The fitted cross talk scale values in the first 5 rows refers the first layer scales, and the last 2 are the middle layer scales. The fit is performed only for the variables with $r^2 > 0.999$.

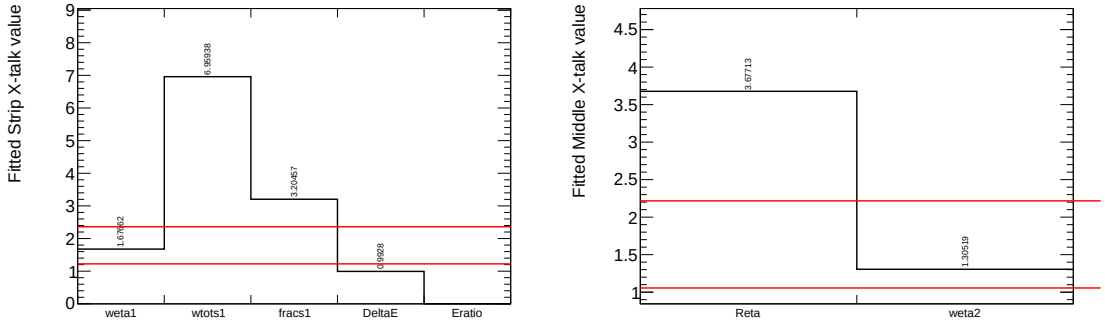

(a) Strip layer

(b) Middle layer

Figure 3.7: Fitted cross talk value from shower shape variables in strip layer (left) and middle layer (right) in $|\eta| \in$[1.20, 1.25]. Red lines are the upper and lower range from the cross talk measurement, i.e. the lower and upper scale values.

	Data FF	Fitted x-talk	r^2
$w_{\eta 1}$	0.017	1.677	1.00
w_{stot}	0.104	6.959	1.00
f_{side}	0.028	3.204	1.00
ΔE	0.000	0.993	1.00
E_{ratio}	-0.003	-	0.99
R_{η}	-0.005	3.677	1.00
$w_{\eta 2}$	0.000	1.305	1.00

Table 3.6: The data fudge factor, the fitted cross talk amplitude scale values from the fudge factor and the linear relationship of different shower shape variables in $|\eta| \in$[1.20, 1.25]. The fitted cross talk scale values in the first 5 rows refers the first layer scales, and the last 2 are the middle layer scales. The fit is performed only for the variables with $r^2 > 0.999$.

4 Material density impact to the shower shapes

As discussed in Sec 1, another important source of the disagreement is the mismodeling of geometry in the simulation. Also this may explain the ϕ direction shower shapes that the cross-talk can not. Before confirming if there is indeed mismodeling in the ATLAS LAr calorimeter, it is worth and convenient to firstly study the possible influence by varying the simulation. Considering the complexity of changing the volume in the geometry description, the variation is done by modifying the material density. Three options are investigated regarding to possible mismodeling:

- Mismodeling of the total weight: increase lead plate density 4%.
- Mismodeling of the plate thickness: decrease LAr density 3%.
- Mismodeling of the plate corner structure: decrease corner lead density 40%.

Besides, three more geometries are used to investigate the impact from the material before the LAr calorimeter:

- Config A (*ATLAS-R2-2016-01-00-02*): 5% ID material scaling.
- Config IBL (*ATLAS-R2-2016-01-00-03*): 10% IBL material scaling.
- Config PP0 (*ATLAS-R2-2016-01-00-04*): 25% PP0 services scaling

1000 particle gun photon events with energy 65.536 GeV, $|\eta| \in [0.2, 0.25]$ are generated and simulated with above detector geometry options. The digitization and reconstruction follow the default configurations. The reconstructed photon energy is first checked to ensure the success modification on the geometry, and are shown in Figure 4.1. In three geometry configurations with material variation before the calorimeter, there is no significant energy shift. The expected energy shift due to the calorimeter material can be calculated from the composite material budget fractions: 18.5% of LAr, 66.7% of lead (6.33% of corner part and 60.35% of straight part) and 14.8% of steel in the LAr EM barrel. Considering the calibration strategies are not changed, the expected relative shift values are -2.6%, -2.4% and 2.6% for 3 self-defined configurations. These values from the simulation are -2.3%, 2.10% and 2.12%, meaning we successfully changed the material in the simulaiton, and the absorber is modified as expected. The abnormal shift when modifing the LAr density is not fully understood yet. After the check the mean value of shower shape variables $w_{\eta 1}$, $w_{\eta 2}$, R_η and R_ϕ are shown in Figure 4.2. All of the 6 configurations contribute very little impact on the shower shapes.

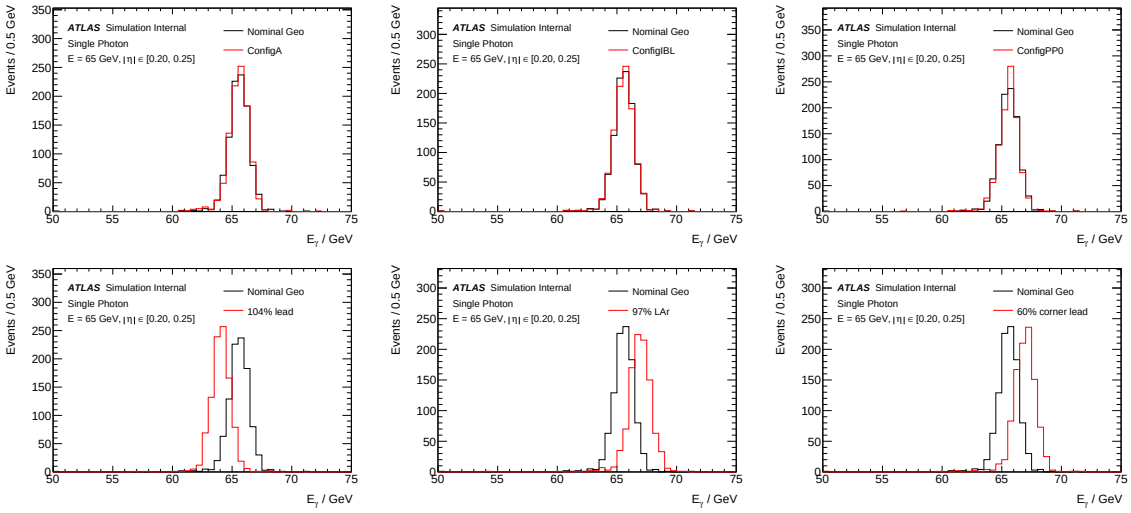

Figure 4.1: Single photon energy distribution for different configurations, comparing with the nominal simulation.

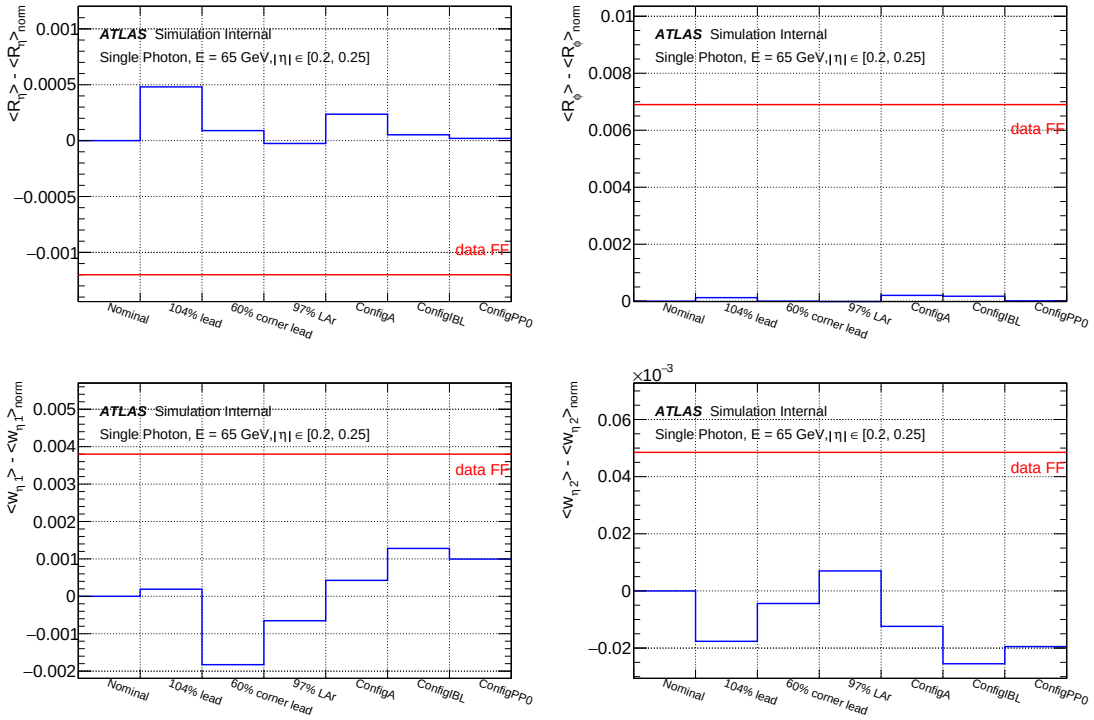

Figure 4.2: Mean values of shower shape variables R_η, R_ϕ, $w_{\eta 1}$ and $w_{\eta 2}$ in $|\eta| \in [0.2, 0.25]$.

5 Summary and conclusion

This note presents the shower shape variation from the impact of cross talk and detector geometry. The modeling of cross talk in the digitization of LAr EM calorimeter is observed to be different from the data. To correct this a set of scale factors are applied into the cross talk amplitude, and the statistical uncertainties from the data are used as the uncertainty of scaling. After the reconstruction, the η direction photon shower shape variables show significant variations, while the attempt of deriving the cross talk amplitude from the measured shower shape variables in data can not give an uniform result. This means the cross talk can be one of the reason for the shower shape mismodeling, but not the only one. The ATLAS LAr detector is re-investigated by comparing the records in ATLAS TDR and the model used in the simulation. The considered parts are the potential mismodeling of material and thickness of the lead absorber, and the imperfect description of the lead plate corner. Modifying them can not give a notable change on the shower shapes. Three more ATLAS detector models used for the systematic study are investigated, which do not show impact on the shower shapes either.

The final explanation of the mismodeling awaits more specific studies. The ϕ direction shape R_ϕ can be hardly changed from known sources, so this is relatively clean to investigate the impact from new sources. Any news can be a good progress. The η direction shape is complex and needs careful treatment.

Bibliography

[1] ATLAS Collaboration, *Electron and photon performance measurements with the ATLAS detector using the 2015–2017 LHC proton–proton collision data*, JINST **14** (2019) P12006, arXiv: 1908.00005 [hep-ex] (cit. on p. 3).

[2] GEANT4 Collaboration, S. Agostinelli et al., *GEANT4 – a simulation toolkit*, Nucl. Instrum. Meth. A **506** (2003) 250 (cit. on pp. 3, 6).

[3] J. Colas et al., *Crosstalk in the ATLAS Electromagnetic Calorimeter; preliminary version*, tech. rep., CERN, 1999, URL: http://cds.cern.ch/record/683952 (cit. on p. 6).

[4] F. Hubaut, B. Laforge, D. Lacour and F. Orsini, *Test Beam Measurement of the Crosstalk in the EM Barrel Module 0*, tech. rep., CERN, 2000, URL: http://cds.cern.ch/record/684055 (cit. on p. 6).

[5] O. Kivernyk, *Measurement of the W boson mass with the ATLAS detector*, Presented 19 Sep 2016, 2017, URL: https://cds.cern.ch/record/2262454 (cit. on p. 6).

The supporting notes for the analysis should also contain a list of contributors. This information should usually be included in `mydocument-metadata.tex`. The list should be printed either here or before the Table of Contents.

List of contributions

Appendices

In an ATLAS note, use the appendices to include all the technical details of your work that are relevant for the ATLAS Collaboration only (e.g. dataset details, software release used). This information should be printed after the Bibliography.